

## **Supplementary Information for the manuscript**

The Supplementary Information contains: Section S1, Figures S1 – S5 and Tables S1 & S2

## **Supplementary**

### **Section S1: Soil Core Saturation and Pore water Extraction**

#### *Soil Core Saturation*

The pore water extraction procedure involved two main steps: peatsoil saturation followed by pore water extraction using the extraction experiment setup (a suction plate system that consists of a pF pressure stage module and pF suction plates; ecoTech Umwelt-Meßsysteme GmbH). To saturate the soil, the white cap was first removed from the blunt end of the soil core. The blunt side of the core was covered with filter paper and capped with a sieve cover. Then, the soil core was flipped, and the white cap was removed from the cutting-edge end of the soil core. To mimic natural infiltration, cores were placed upside down in cylindrical containers (i.e., the blunt side was placed down while the cutting edge faced upwards). Deionised water was incrementally added every 24 hours for four days to achieve gradual saturation to ensure uniform moisture distribution. Care was taken to avoid pouring water on the top surface of the soil core to prevent air entrapment. During the saturation period, the cylinders were placed in a dark rectangular container and covered with a cap placed on top of the cutting edge to prevent evaporation and protect the soil from solar radiation (Shokrana and Ghane 2020). Although deionised water has been shown to cause pore structure changes and reduce  $K_s$  in bog peat due to pore constriction (Kettridge and Binley 2010), Gosch et al. (2018) observed no such effects in degraded fen peat from Pölchow. Their results suggest that, for this peat type, low salinity conditions do not significantly alter pore structure or hydraulic conductivity.

### *Porewater Extraction*

Porewater extraction was conducted using a suction plate system designed to simulate matric potentials under controlled laboratory conditions. The system, illustrated in Supplementary Figure S2, consisted of eight circular borosilicate glass suction plates (ecoTech UmweltMeßsysteme GmbH, Germany; diameter: 7.5 cm), each fitted with a 10- $\mu$ m membrane filter and connected to PTFE tubing. These plates were positioned within a sealed container box and connected to a precision-controlled vacuum system called a pF pressure stage module (ecoTech Umwelt-Meßsysteme GmbH). The suction system served dual functions: (i) applying constant negative pressure to extract pore water from the soil cores and (ii) directing the extracted water to collection bottles via the tubing network.

The pF pressure stage module allows pressure to be adjusted between the range of - 60 to - 750 hPa with an accuracy of  $\pm 1$  hPa. In this experiment, - 60hPa was initially applied for four days followed by - 600 hPa for another four days to drain pore water from the macro- and mesopore size domains. We estimated the applied negative pressures using the capillary rise equation (Bear 1972):

$$h = \frac{2\gamma \cos \theta}{\rho g r} \quad (1)$$

where  $r$  is the pore radius (cm),  $\gamma$  is the surface tension of water (72.7 dyn cm<sup>-1</sup>),  $\theta$  is the soil liquid contact angle (°),  $\rho$  is the density of water (1.0 g cm<sup>-3</sup>),  $g$  is the acceleration of gravity (980 cm s<sup>-2</sup>), and  $h$  is the water pressure head (- cm H<sub>2</sub>O). The contact angle was reported to range from

40° to 52° for moderately hydrophobic organic soils and peat (Carey et al. 2007; Gharedaghloo and Price 2018; Bachmann et al. 2003).

Varying class limits are used to define pore size domains. Reported class limits of the equivalent diameter ( $\mu\text{m}$ ) of macropores range between 30  $\mu\text{m}$  and 5000  $\mu\text{m}$  for macropores and approximately 0.2 to 30  $\mu\text{m}$  for mesopores (Beven and Germann 1982; Cameron and Buchan 2006; Carter et al. 1994). In this study, we used a modified pore size classification from Tassinari et al. (2022) which included macropores (equivalent pore diameter > 30  $\mu\text{m}$ ), mesopores (equivalent pore diameter 3 - 30  $\mu\text{m}$ ) and micropores (equivalent pore diameter 0.2 - 3  $\mu\text{m}$ ).

We set the soil liquid contact angle was set to 52° for peat, as recommended by Gharedaghloo and Price (2019). Thus, the applied tensions of - 60 hPa and - 600 hPa were estimated to correspond to pore radii of approximately 30  $\mu\text{m}$  and ca.3  $\mu\text{m}$ , respectively.

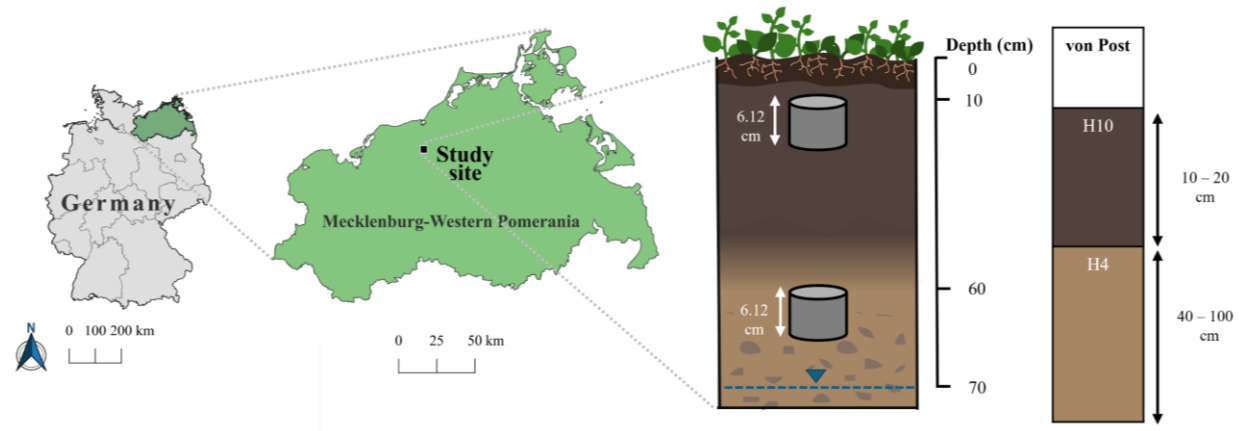


**Figure S1:** study site in Pölchow (right pane showing soil core sampling depths). The groundwater table at the study site ranged between 70 - 75 cm bgl (below ground level). Following von Post (1922), the topsoil was classified as severely degraded (H10) and the subsoil as moderately degraded (H4).

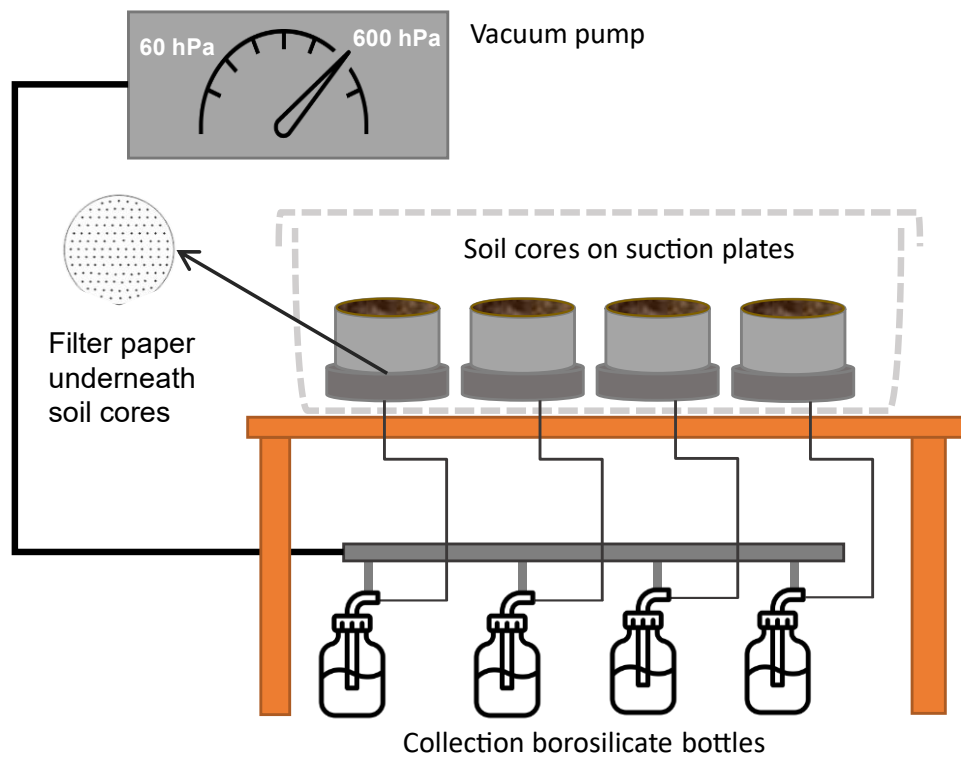


**Figure S2:** Experimental setup for the leaching experiment. Eight borosilicate glass suction plates (EcoTech Bonn; 7.5 cm diameter; 10- $\mu$ m membrane filter; PTFE tubing) were arranged in a container box and connected to a vacuum system for pore water collection and pressure regulation. The system operated at -60 hPa, followed by -600 hPa for four days, respectively.

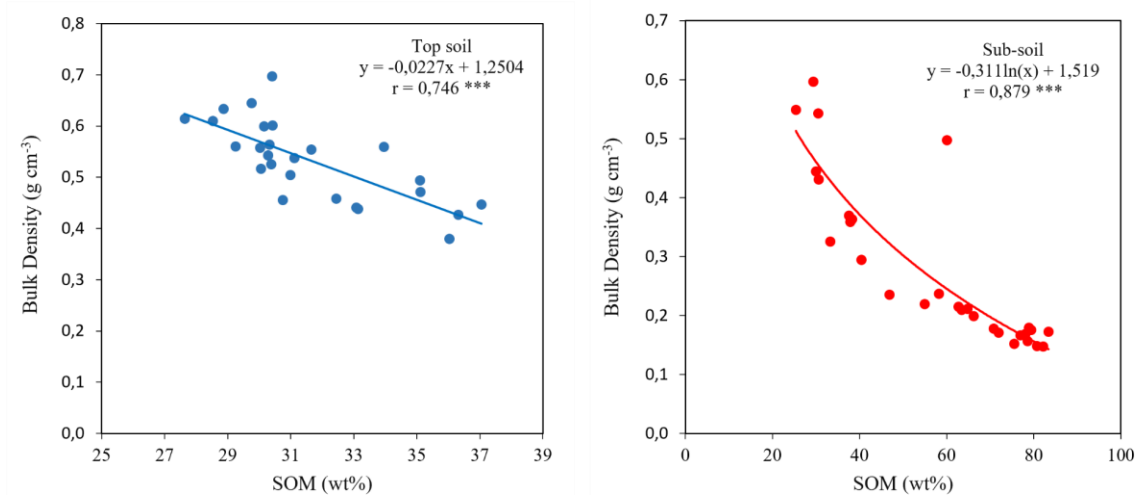


**Figure S3:** Relationship of soil organic matter (SOM; wt%) content and bulk density (BD; g cm<sup>-3</sup>) from the top- and sub-soil domains.

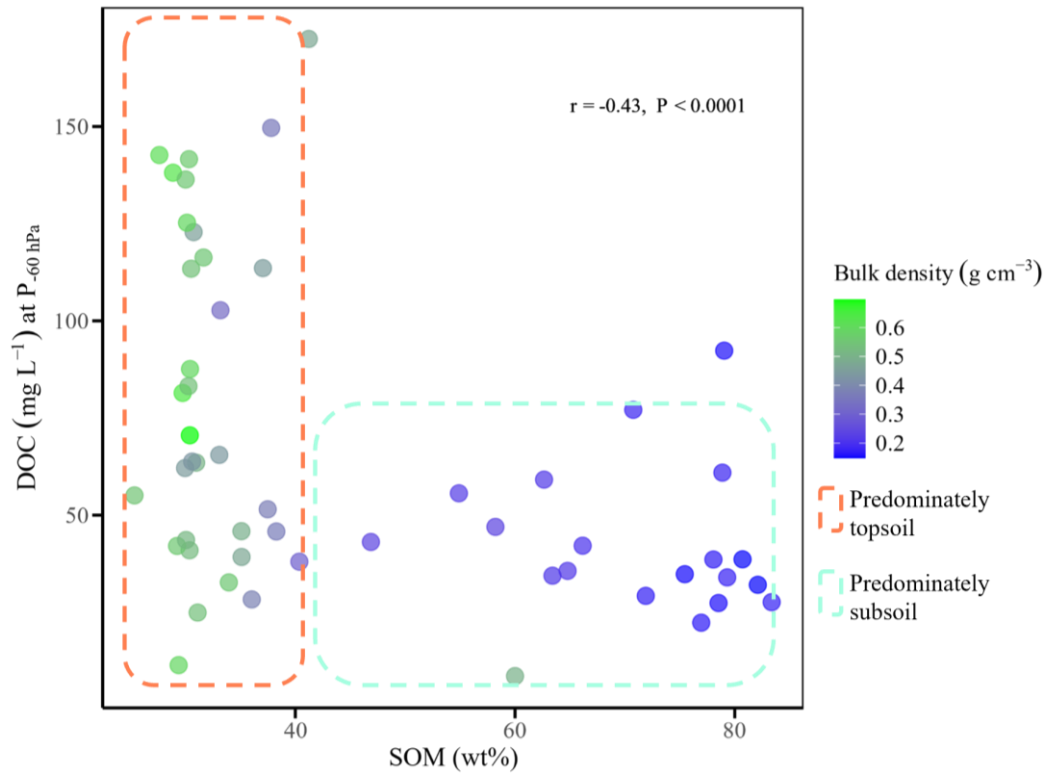


**Figure S4:** Relationship between DOC concentration at - 60 hPa and SOM content ( $r = - 0.43$ ;  $p < 0.0001$ ). Observation points are colour-coded by bulk density, serving as a proxy degradation state of peat soil.

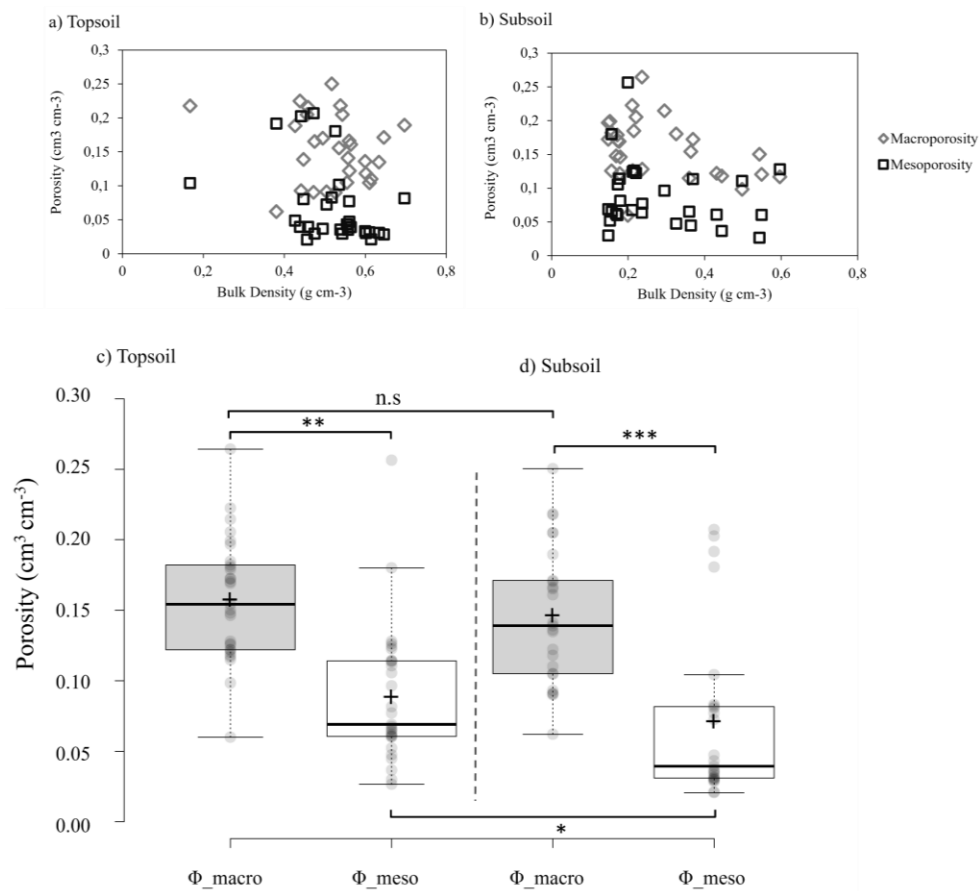


**Figure S5:** The relationship between bulk density and porosity from the (a) topsoil and (b) subsoil depths. The grey diamonds represent macroporosity and the black squares, mesoporosity. The box plots represent the distribution of macro- and mesoporosity at topsoil (c) and subsoil (d) depths. The asterisk denotes a significant difference in porosity between the groups (\*\* $p < 0.01$ ; \*\*\* $p < 0.001$ ), while “n.s” indicates no significant difference.



**Table S1:** Soil and DOC variables from the top- and subsoil peat samples along with their descriptive statistics.

	Soil Depth	Minimum	Maximum	Mean	Median	Standard Deviation	CV
DOC <sub>-60 hPa</sub> (mg L <sup>-1</sup> )	Topsoil	24.94	172.54	85.46	82.33	43.89	51.35
DOC <sub>-600 hPa</sub> (mg L <sup>-1</sup> )		24.75	195.17	107.63	96.91	43.67	40.58
SOM (wt%)		22.48	79.04	33.29	30.74	9.46	28.43
Total porosity (cm <sup>3</sup> cm <sup>-3</sup> )		0.66	0.89	0.75	0.74	0.04	6.00
Dry Bulk Density (g cm <sup>-3</sup> )		0.16	0.70	0.52	0.54	0.10	19.69
Macroporosity (cm <sup>3</sup> cm <sup>-3</sup> )		0.06	0.25	0.15	0.14	0.05	28.75
Mesoporosity (cm <sup>3</sup> cm <sup>-3</sup> )		0.02	0.21	0.05	0.04	0.06	49.74
DOC <sub>-60 hPa</sub> (mg L <sup>-1</sup> )	Subsoil	8.59	149.66	49.72	42.14	30.04	70.93
DOC <sub>-600 hPa</sub> (mg L <sup>-1</sup> )		17.29	161.33	48.68	41.07	28.41	70.17
SOM (wt%)		25.36	83.36	57.45	62.64	19.90	34.64
Total porosity (cm <sup>3</sup> cm <sup>-3</sup> )		0.59	0.90	0.81	0.85	0.10	11.93
Dry Bulk Density (g cm <sup>-3</sup> )		0.15	0.60	0.28	0.21	0.14	49.41
Macroporosity (cm <sup>3</sup> cm <sup>-3</sup> )		0.06	0.26	0.16	0.15	0.04	27.74
Mesoporosity (cm <sup>3</sup> cm <sup>-3</sup> )		0.03	0.26	0.08	0.07	0.05	45.57

**Table S2:** Spearman's rank correlation matrix between dissolved organic matter (DOC) concentrations at - 60 hPa and - 600 hPa, soil organic matter (SOM), total porosity ( $\Phi_{\text{total}}$ ), dry bulk density, macroporosity ( $\Phi_{\text{macro}}$ ), and mesoporosity ( $\Phi_{\text{meso}}$ ). The entire observation dataset (i.e., topsoil and subsoil) was used to perform the analysis.

	<b>- 60 hPa DOC (mg L<sup>-1</sup>)</b>	<b>- 600 hPa DOC (mg L<sup>-1</sup>)</b>	<b>SOM (wt%)</b>	<b><math>\Phi_{\text{total}}</math> (cm<sup>3</sup> cm<sup>-3</sup>)</b>	<b>Bulk Density (g cm<sup>-3</sup>)</b>	<b><math>\Phi_{\text{macro}}</math> (cm<sup>3</sup> cm<sup>-3</sup>)</b>	<b><math>\Phi_{\text{meso}}</math> (cm<sup>3</sup> cm<sup>-3</sup>)</b>
- 60 hPa DOC (mg L <sup>-1</sup> )	1						
- 600 hPa DOC (mg L <sup>-1</sup> )	0,75	1					
SOM (wt%)	-0,46	-0,52	1				
$\Phi_{\text{total}}$ (cm <sup>3</sup> cm <sup>-3</sup> )	-0,33	-0,40	0,84	1			
Bulk Density (g cm <sup>-3</sup> )	0,44	0,57	-0,89	-0,90	1		
$\Phi_{\text{macro}}$ (cm <sup>3</sup> cm <sup>-3</sup> )	-0,12	-0,16	0,21	0,28	-0,26	1	
$\Phi_{\text{meso}}$ (cm <sup>3</sup> cm <sup>-3</sup> )	-0,44	-0,31	0,19	0,24	-0,26	-0,42	1

$\theta$

## References

Bachmann, J.; Woche, S. K.; Goebel, M.-O.; Kirkham, M. B.; Horton, R. (2003): Extended methodology for determining wetting properties of porous media. In *Water Resour. Res.* 39 (12). DOI: 10.1029/2003WR002143.

Bear, Jacob (1972): *Dynamics of Fluids in Porous Media*. New York, NY: American Elsevier Publishing Company, Inc.

Beven, Keith; Germann, Peter (1982): Macropores and water flow in soils. In *Water Resour. Res.* 18 (5), pp. 1311–1325. DOI: 10.1029/WR018i005p01311.

Cameron, Keith C.; Buchan, Graeme D. (2006): Porosity and pore size distribution. In *Encyclopedia of soil science* 2, pp. 1350–1353.

Carey, Sean K.; Quinton, William L.; Goeller, Neil T. (2007): Field and laboratory estimates of pore size properties and hydraulic characteristics for subarctic organic soils. In *Hydrol. Process.* 21 (19), pp. 2560–2571.

Carter, M. R.; Kunelius, H. T.; Angers, D. A. (1994): Soil Structural Form and Stability, and Organic Matter under Cool-Season Perennial Grasses. In *Soil Science Society of America Journal* 58 (4), pp. 1194–1199. DOI: 10.2136/sssaj1994.03615995005800040027x.

ecoTech Umwelt-Meßsysteme GmbH: Extraction of soil solution with ecoTech suction plates: Manual. Bonn, Germany: ecoTech Umwelt-Meßsysteme GmbH. Available online at <https://www.vanwalt.com/pdf/information-sheets/ecoTech-Manual-Suction-plates.pdf>.

Gharedaghloo, Behrad; Price, Jonathan S. (2018): Fate and transport of free-phase and dissolved-phase hydrocarbons in peat and peatlands: developing a conceptual model. In *Environmental Reviews* 26 (1), pp. 55–68. DOI: 10.1139/er-2017-0002.

Gharedaghloo, Behrad; Price, Jonathan S. (2019): Characterizing the immiscible transport properties of diesel and water in peat soil. In *Journal of Contaminant Hydrology* 221, pp. 11–25. DOI: 10.1016/j.jconhyd.2018.12.005.

Gosch, Lennart; Janssen, Manon; Lennartz, Bernd (2018): Impact of the water salinity on the hydraulic conductivity of fen peat. In *Hydrological Processes* 32 (9), pp. 1214–1222. DOI: 10.1002/hyp.11478.

Kettridge, Nicholas; Binley, Andrew (2010): Evaluating the effect of using artificial pore water on the quality of laboratory hydraulic conductivity measurements of peat. In *Hydrol. Process.* 24 (18), pp. 2629–2640. DOI: 10.1002/hyp.7693.

Shokrana, Md Sami Bin; Ghane, Ehsan (2020): Measurement of soil water characteristic curve using HYPROP2. In *MethodsX* 7, p. 100840. DOI: 10.1016/j.mex.2020.100840.

Tassinari, Diego; Soares, Pablo G. S.; Costa, Camila R.; Barral, Uidemar M.; Horák-Terra, Ingrid; Silva, Alexandre C.; Carmo, William J. (2022): Water Retention and Pore Size Distribution in Organic Soils From Tropical Mountain Peatlands Under Forest and Grassland. In *Mires and Peat* 28, p. 12. DOI: 10.19189/MaP.2022.OMB.StA.2374.

von Post, Lennart (1922): Sveriges geologiska undersöknings torvinventering och några av dess hittills vunna resultat. In *Svenska Mosskulturföreningens Tidskrift* 36, pp. 1–37.